Improved Spherical Wave Least Squares Method for Analyzing Periodic Arrays of Spheres

Huan Xie[1,2,3] and Ya Yan Lu[3]

[1] *Joint Advanced Research Center of University of Science and Technology of China and City University of Hong Kong, Suzhou, Jiangsu, China*

[2] *Department of Mathematics, University of Science and Technology of China Hefei, Anhui, China*

[3] *Department of Mathematics, City University of Hong Kong, Kowloon, Hong Kong*

For analyzing plane wave scattering from a multilayer periodic structure where each layer consists of a two-dimensional periodic array of spheres, a spherical wave least squares method is developed which extends and improves the earlier work by Matsushima *et al.* (Progress in Electromagnetics Research, vol. 69, pp. 305-322, 2007). A number of techniques are used to speed up the method and to reduce the memory requirement. Spherical wave expansions are used in one unit cell containing a sphere in each layer, and quasi-peridic conditions are imposed on lateral surfaces of the unit cell in the least squares sense. Unlike the layer-KKR method (A. Modinos, Physica A, vol. 141, pp. 575-588, 1987), the method does not need lattice sums and it is relatively simple to implement.

OCIS codes: 000.4430, 050.1755.

1. Introduction

In the last two decades, photonic crystals (PhCs) [1] have been extensively studied both theoretically and experimentally, since they exhibit bandgaps and other unusual properties that can be used to control and manipulate light. Three-dimensional (3D) PhCs are structures with three linearly independent periodic directions where the periods are on the scale of the optical wavelength. Although 3D PhCs are more difficult to fabricate than two-dimensional (2D) PhCs having two periodic directions, they have potential applications in developing ultrahigh quality-factor microcavities and zero-threshold lasers. In particular, complete bandgaps that prohibit propagating waves in all directions can only exist in 3D PhCs [2–5]. A periodic assembly of dielectric or air spheres in a host medium gives rise to a relatively simple 3D PhC. In fact, a complete bandgap was first found in a 3D PhC composed of spheres on a diamond lattice [2].

While the band structure is the most fundamental property of a PhC, it is also important to calculate the transmission and reflection spectra for a PhC with a finite thickness. For 3D PhCs involving dielectric or air spheres, this is a scattering problem for plane waves incident upon a multilayer structure where each layer is a 2D periodic array of spheres. Such a multiple scattering problem has been studied before the wide spread interest on PhCs [6,7]. The methods presented in these earlier studies are extensions to electromagnetic waves of the classical multipole method for scalar multiple scattering problems [8], they are related to the exact spherical wave solutions of Mie and Debye for a single sphere [9]. The method was called layer-KKR or vector-KKR (Korringa-Kohn-Rostoker) by the authors and was further extended and enhanced in [10–14]. To account for the infinite number of spheres in each layer, the layer-KKR method requires sophisticated lattice sums techniques. Meanwhile, the scattering problems for a 3D PhC of finite thickness and a crossed diffraction grating are identical mathematically. Therefore, many existing numerical methods for diffraction gratings, such as the Fourier modal method [15], the finite element method [16] and the differential method [17], can be used to calculate the transmission and reflection spectra for finite PhCs. Unfortunately, these general methods are not very efficient for analyzing 3D PhCs. The Fourier modal method must approximate the boundaries of the spheres by staircase approximations which have limited accuracy. The finite element method gives rise to large, complex, indefinite and sparse linear systems that are expensive to solve. The differential method reduces the original problem to a boundary value problem for a large system of ordinary differential equations, but the boundary value problem is still expensive to solve. Clearly, to analyze 3D PhCs involving spherical structures, it is advantageous to use spherical wave expansions as in the layer-KKR method, and it is also desirable to avoid the relatively complicated lattice sums.

In a recent paper [18], Matsushima *et al.* developed a spherical wave least squares method for analyzing plane wave scattering by multilayer periodic arrays of spheres on a simple cubic lattice, using spherical wave expansions. The lattice sums are avoided, since the electromagnetic field components around each sphere are required to satisfy the quasi-periodic conditions in the periodic conditions. In this paper, we improve the spherical wave least squares method in a number of aspects. Using a preprocessing step, a new ordering strategy and a new solution technique, we are able to reduce the computational complexity and the memory requirement significantly. Since a periodic structure with a cubic lattice of spherical inclusions is a very special structure which does not offer the flexibility needed in practical applications, we extend the spherical wave least squares method to more general structures where the spheres in each layer are located on an arbitrary 2D lattice and they are allowed to have arbitrary shifts in different layers.

2. Problem formulation

We consider a periodic structure bounded by two homogeneous media given in $z < 0$ and $z > D$, respectively, where $D > 0$ and $\{x, y, z\}$ is a Cartesian coordinate system. Let ε and μ be the relative permittivity (dielectric constant) and the relative magnetic permeability of the structure, then ε and μ are real constants $\{\varepsilon^{(1)}, \mu^{(1)}\}$ and $\{\varepsilon^{(2)}, \mu^{(2)}\}$ for $z > D$ and $z < 0$, respectively. For $0 < z < D$, the structure is periodic in two directions parallel to the xy plane. Let $\mathbf{a}_1$ and $\mathbf{a}_2$ be two primitive translation vectors of the periodic structure, then

$$\begin{aligned} \varepsilon(\mathbf{x} + l_1\mathbf{a}_1 + l_2\mathbf{a}_2, z) &= \varepsilon(\mathbf{x}, z), \\ \mu(\mathbf{x} + l_1\mathbf{a}_1 + l_2\mathbf{a}_2, z) &= \mu(\mathbf{x}, z), \end{aligned}$$

where $\mathbf{x} = (x, y)$, l_1 and l_2 are arbitrary integers. We also assume that the periodic structure consists of Q layers separated by

$$0 = z_0 < z_1 < ... < z_Q = D.$$

The q-th layer given by $z_{q-1} < z < z_q$ contains identical spheres with their centers at

$$(\mathbf{s}_q + l_1\mathbf{a}_1 + l_2\mathbf{a}_2,\ z_{q-1/2}),$$

where l_1 and l_2 are integers, $\mathbf{s}_q$ is a common shift of the centers with respect to the standard lattice points defined by $\mathbf{a}_1$ and $\mathbf{a}_2$, and $z_{q-1/2} \in (z_{q-1}, z_q)$. In each layer, the medium outside the spheres is assumed to be homogeneous. For different layers, the spheres and the media surrounding the spheres can be different.

Assuming the time dependence is $\exp(-i\omega t)$, where ω is the angular frequency, the electromagnetic field satisfies the following Maxwell's equations:

$$\nabla \times \mathbf{E} = ik_0\mu\tilde{\mathbf{H}}, \quad \nabla \times \tilde{\mathbf{H}} = -ik_0\varepsilon\mathbf{E}, \tag{1}$$

where $\tilde{\mathbf{H}} = \sqrt{\mu_0/\varepsilon_0}\mathbf{H}$ is a scaled magnetic field, $k_0 = \omega/c$ is the free space wavenumber, c is the speed of light in vacuum, ε_0 and μ_0 are the permittivity and permeability in vacuum. To simplify the notations, we denote $\tilde{\mathbf{H}}$ by $\mathbf{H}$ in the rest of this paper.

In the top region, $z > D$, we specify an incident wave with a wavevector $\mathbf{k}^{(i)} = (\vec{\alpha}_{00}, -\gamma_{00}^{(1)})$, where $\vec{\alpha}_{00}$ is a vector for the first two components of the wavevector and $\gamma_{00}^{(1)}$ satisfies

$$\gamma_{00}^{(1)} = \sqrt{k_0^2\varepsilon^{(1)}\mu^{(1)} - |\vec{\alpha}_{00}|^2} > 0.$$

For a given wavevector, there are only two linearly independent plane waves. Therefore, an incident wave with a normalized electric field can be written as

$$\begin{aligned} \begin{bmatrix} \mathbf{E}^{(i)} \\ \mathbf{H}^{(i)} \end{bmatrix} &= \begin{bmatrix} \mathbf{n}^{(i)} & \mathbf{t}^{(i)} \\ -\rho^{(1)}\mathbf{t}^{(i)} & \rho^{(1)}\mathbf{n}^{(i)} \end{bmatrix} \begin{bmatrix} \cos\delta \\ \sin\delta \end{bmatrix} \\ &\quad \exp[i(\vec{\alpha}_{00} \cdot \mathbf{x} - \gamma_{00}^{(1)} z)], \end{aligned} \tag{2}$$

where $\rho^{(1)} = \sqrt{\varepsilon^{(1)}/\mu^{(1)}}$, δ is the polarization angle, $\mathbf{n}^{(i)}$ and $\mathbf{t}^{(i)}$ are unit vectors normal and tangential to the incident plane, respectively. The incident plane is spanned by the wavevector and the z-axis. Let $\hat{\mathbf{k}}^{(i)}$ and $\hat{\mathbf{z}}$ be the unit vectors in the directions of the incident wavevector and the positive z axis, respectively, then

$$\mathbf{n}^{(i)} = \frac{\hat{\mathbf{k}}^{(i)} \times \hat{\mathbf{z}}}{|\hat{\mathbf{k}}^{(i)} \times \hat{\mathbf{z}}|}, \quad \mathbf{t}^{(i)} = \mathbf{n}^{(i)} \times \hat{\mathbf{k}}^{(i)}.$$

For normal incidence, i.e., $\vec{\alpha}_{00} = (0, 0)$, we let $\mathbf{n}$ be the unit vector in the positive x direction.

The incident wave gives rise to a reflected wave for $z > D$ and a tranmitted wave for $z < 0$. Since the structure is periodic in the xy plane, the reflected and transmitted waves can be expanded in plane waves. From the primitive translation vectors $\mathbf{a}_1$ and $\mathbf{a}_2$, we have the reciprocal vectors $\mathbf{b}_1$ and $\mathbf{b}_2$ satisfying

$$\mathbf{a}_j \cdot \mathbf{b}_l = \begin{cases} 1 & \text{if } j = l, \\ 0 & \text{if } j \neq l, \end{cases}$$

then the wavevectors of the reflected and transmitted plane waves are $\mathbf{k}_{jk}^{(r)} = (\vec{\alpha}_{jk}, \gamma_{jk}^{(1)})$ and $\mathbf{k}_{jk}^{(t)} = (\vec{\alpha}_{jk}, -\gamma_{jk}^{(2)})$, respectively, where

$$\begin{aligned} \vec{\alpha}_{jk} &= \vec{\alpha}_{00} + 2\pi j \mathbf{b}_1 + 2\pi k \mathbf{b}_2, \\ \gamma_{jk}^{(1)} &= \sqrt{k_0^2 \varepsilon^{(1)} \mu^{(1)} - |\vec{\alpha}_{jk}|^2}, \\ \gamma_{jk}^{(2)} &= \sqrt{k_0^2 \varepsilon^{(2)} \mu^{(2)} - |\vec{\alpha}_{jk}|^2}. \end{aligned}$$

Since there are two linearly independent plane waves for each wavevector, we expand the reflected and transmitted plane waves as

$$\begin{aligned} \begin{bmatrix} \mathbf{E}^{(r)} \\ \mathbf{H}^{(r)} \end{bmatrix} &= \sum_{jk} \begin{bmatrix} \mathbf{n}_{jk}^{(r)} & \mathbf{t}_{jk}^{(r)} \\ -\rho^{(1)} \mathbf{t}_{jk}^{(r)} & \rho^{(1)} \mathbf{n}_{jk}^{(r)} \end{bmatrix} \mathbf{R}_{jk} \\ &\quad \exp[i(\vec{\alpha}_{jk} \cdot \mathbf{x} - \gamma_{jk}^{(1)} z)], \qquad (3) \\ \begin{bmatrix} \mathbf{E}^{(t)} \\ \mathbf{H}^{(t)} \end{bmatrix} &= \sum_{jk} \begin{bmatrix} \mathbf{n}_{jk}^{(t)} & \mathbf{t}_{jk}^{(t)} \\ -\rho^{(2)} \mathbf{t}_{jk}^{(t)} & \rho^{(2)} \mathbf{n}_{jk}^{(t)} \end{bmatrix} \mathbf{T}_{jk} \\ &\quad \exp[i(\vec{\alpha}_{jk} \cdot \mathbf{x} - \gamma_{jk}^{(2)} z)], \qquad (4) \end{aligned}$$

where $\mathbf{R}_{jk}$ and $\mathbf{T}_{jk}$ are column vectors of length two,

$$\hat{\mathbf{k}}_{jk}^{(r)} = \frac{(\vec{\alpha}_{jk}, \gamma_{jk}^{(1)})}{k_0 \sqrt{\varepsilon^{(1)} \mu^{(1)}}}, \quad \hat{\mathbf{k}}_{jk}^{(t)} = \frac{(\vec{\alpha}_{jk}, -\gamma_{jk}^{(2)})}{k_0 \sqrt{\varepsilon^{(2)} \mu^{(2)}}},$$

and

$$\begin{aligned} \mathbf{n}_{jk}^{(r)} &= \frac{\hat{\mathbf{k}}_{jk}^{(r)} \times \hat{\mathbf{z}}}{|\hat{\mathbf{k}}_{jk}^{(r)} \times \hat{\mathbf{z}}|}, \quad \mathbf{n}_{jk}^{(t)} = \frac{\hat{\mathbf{k}}_{jk}^{(t)} \times \hat{\mathbf{z}}}{|\hat{\mathbf{k}}_{jk}^{(t)} \times \hat{\mathbf{z}}|}, \\ \mathbf{t}_{jk}^{(r)} &= \mathbf{n}_{jk}^{(r)} \times \hat{\mathbf{k}}_{jk}^{(r)}, \quad \mathbf{t}_{jk}^{(t)} = \mathbf{n}_{jk}^{(t)} \times \hat{\mathbf{k}}_{jk}^{(t)}. \end{aligned}$$

Our objective is to calculate the vector coefficients $\mathbf{R}_{jk}$ and $\mathbf{T}_{jk}$ for a given incident wave.

3. The least squares problem

A least squares method based on spherical wave expansions was developed by Matsushima *et al.* [18] for periodic arrays of spheres on a simple cubic lattice. In this section, we present an improved method for spheres on more general lattices including possible shift of the sphere centers in different layers. The main idea is quite simple. For a multilayer of spheres, we identify a cylindrical unit cell for each layer, express the electromagnetic field in the unit cell in a spherical wave expansion, then enforce quasi-periodic conditions on the lateral boundaries of the unit cells and continuity conditions on horizontal interfaces between the layers. These conditions are enforced in the least squares sense. This allows us to determine the coefficients of the spherical waves in the unit cells, as well as the reflection and transmission coefficients.

For the q-th layer given by $z_{q-1} < z < z_q$, we define the unit cell Ω_q as a cylinder with a cross section S_q surrounding the central sphere located at $(\mathbf{s}_q, z_{q-1/2})$, namely

$$\Omega_q = \{(\mathbf{x}, z) \,:\, \mathbf{x} \in S_q,\ z_{q-1} < z < z_q\}.$$

For better convergence of spherical wave expansions in Ω_q, the cross section S_q is chosen to be the set of points (on the xy plane) that cannot be brought closer to $\mathbf{s}_q$ by any integer translations in $\mathbf{a}_1$ or $\mathbf{a}_2$. That is,

$$S_q = \{\mathbf{x} \,:\, |\mathbf{x} - \mathbf{s}_q| \le |\mathbf{x} + l_1\mathbf{a}_1 + l_2\mathbf{a}_2 - \mathbf{s}_q|\}$$

for any integer pair (l_1, l_2). To give a more detailed description for S_q, we assume that $\mathbf{a}_1$ and $\mathbf{a}_2$ satisfy

$$|\mathbf{a}_1| \le |\mathbf{a}_2 \pm \mathbf{a}_1| \quad \text{and} \quad |\mathbf{a}_2| \le |\mathbf{a}_2 \pm \mathbf{a}_1|.$$

There is no loss of generality, since otherwise we can replace $\mathbf{a}_1$ or $\mathbf{a}_2$ (with a longer length) by $\mathbf{a}_2 + \mathbf{a}_1$ or $\mathbf{a}_2 - \mathbf{a}_1$ (with a shorter length). Let $\mathbf{a}_3$ be the shorter vector of $\mathbf{a}_2 + \mathbf{a}_1$ and $\mathbf{a}_2 - \mathbf{a}_1$, then S_q is the domain bounded by three pairs of straight lines:

$$\mathbf{a}_j \cdot (\mathbf{x} - \mathbf{s}_q) = \pm\frac{|\mathbf{a}_j|^2}{2}, \quad j = 1, 2, 3. \tag{5}$$

More precisely, S_q is a hexagon given by

$$S_q = \left\{\mathbf{x} \,:\, |\mathbf{a}_j \cdot (\mathbf{x} - \mathbf{s}_q)| < \frac{|\mathbf{a}_j|^2}{2}, \quad j = 1, 2, 3\right\}.$$

For a square lattice, we have

$$\mathbf{a}_1 = (a, 0), \quad \mathbf{a}_2 = (0, a), \tag{6}$$

where a is the lattice constant, then $\mathbf{a}_3$ can be either $\mathbf{a}_2 + \mathbf{a}_1$ or $\mathbf{a}_2 - \mathbf{a}_1$, but the condition associated with $\mathbf{a}_3$ is redundant, thus S_q becomes a square. In general, if $\mathbf{a}_1$ is perpendicular

to $\mathbf{a}_2$, then $\mathbf{a}_3$ is not needed and S_q is a rectangle. For an equilateral triangular lattice, we have

$$\mathbf{a}_1 = (a, 0),\ \mathbf{a}_2 = \frac{a}{2}(1, \sqrt{3}),\ \mathbf{a}_3 = \frac{a}{2}(-1, \sqrt{3}), \tag{7}$$

where a is the lattice constant, then S_q is a regular hexagon.

Due to the periodicity of the structure and the incident wave, the electromagnetic field satisfies the quasi-peridic conditions. The unit cell Ω_q has three (or two, if $\mathbf{a}_1 \perp \mathbf{a}_2$) pairs of lateral surfaces with their x and y coordinates satisfying (5). That is,

$$\Sigma_{q,j}^{\pm} = \left\{ (\mathbf{x}, z)\ :\ \mathbf{a}_j \cdot (\mathbf{x} - \mathbf{s}_q) = \pm \frac{|\mathbf{a}_j|^2}{2}, z_{q-1} < z < z_q \right\}$$

for $j = 1$, 2, 3. The quasi-periodic condition in the direction $\mathbf{a}_j$ is

$$\mathbf{E}(\mathbf{x} + \mathbf{a}_j, z) = \rho_j \mathbf{E}(\mathbf{x}, z),\ \mathbf{H}(\mathbf{x} + \mathbf{a}_j, z) = \rho_j \mathbf{H}(\mathbf{x}, z), \tag{8}$$

for $(\mathbf{x}, z) \in \Sigma_{q,j}^{-}$, where $\vec{\alpha}_{00}$ is part of the incident wavevector and $\rho_j = \exp(i\vec{\alpha}_{00} \cdot \mathbf{a}_j)$. Of course, the quasi-periodic condition associated with $\mathbf{a}_3$ can be derived from those associated with $\mathbf{a}_1$ and $\mathbf{a}_2$, and it is not needed if $\mathbf{a}_1 \perp \mathbf{a}_2$.

In the unit cell Ω_q, we expand the electromagnetic field in spherical waves using a local spherical coordinate system with the origin located at the center of the sphere, i.e., $(\mathbf{s}_q, z_{q-1/2})$. Each spherical wave is associated with a pair of integers l and m, where $l \geq 1$ and $-l \leq m \leq l$. The integer l is the index of the spherical Bessel functions in the radial variable, and the integer l is associated with a spherical harmonic. However, for each pair (l, m), there are two linearly independent spherical waves. We can choose these two spherical waves such that their radial components of the electric field or the magnetic field are zero, respectively. We denote the coefficients of the spherical wave expansion in Ω_q as $d_{lm,1}^{(q)}$ and $d_{lm,2}^{(q)}$.

For numerical implementation, the spherical wave expansions in the unit cells and the plane wave expansions of the reflected and transmitted waves must be truncated. For the plane waves in (3) and (4), the indices j and k are truncated by $-J_* \leq j, k \leq J_*$. Therefore, we retain $(2J_* + 1)^2$ different wave vectors and $2(2J_* + 1)^2$ different plane waves in (3) or (4). The spherical waves are truncated to $l \leq L_*$. This gives rise to a total of $L_*(L_* + 2)$ index pairs and a total of $2L_*(L_* + 2)$ spherical waves in each unit cell. Typically, we choose $L_* = 3J_*$.

To determine the expansion coefficients, we set up an over-determined system of equations and solve the system as a least squares problem. On the lateral surfaces of the unit cells, we impose the quasi-periodic conditions for the tangential field components. For the pair of surfaces $\Sigma_{q,j}^{-}$ and $\Sigma_{q,j}^{+}$ which are perpendicular to vector $\mathbf{a}_j$, we have

$$\begin{aligned} \mathbf{a}_j \times \mathbf{E}(\mathbf{x} + \mathbf{a}_j, z) &= \rho_j \mathbf{a}_j \times \mathbf{E}(\mathbf{x}, z), \\ \mathbf{a}_j \times \mathbf{H}(\mathbf{x} + \mathbf{a}_j, z) &= \rho_j \mathbf{a}_j \times \mathbf{H}(\mathbf{x}, z), \end{aligned}$$

for $(\mathbf{x}, z) \in \Sigma_{q,j}^-$. Notice that if $\mathbf{x} \in \Sigma_{q,j}^-$, then $\mathbf{x} + \mathbf{a}_j \in \Sigma_{q,j}^+$. On the surface $\Sigma_{q,j}^-$, we choose $N_j \times N_z$ points based on a uniform discretization of corresponding edge of S_q by N_j points and a uniform discretization of the interval (z_{q-1}, z_q) by N_z point. Therefore, we have a total of $4N_tN_z$ quasi-periodic conditions, where $N_t = N_1 + N_2 + N_3$. For the square lattice (6), we have $N_1 = N_2$ and $N_3 = 0$. To maintain a uniform distribution of sampling points, we requie $N_1 \approx aN_z/(z_q - z_{q-1})$. For the equilateral triangular lattice (7), we have $N_1 = N_2 = N_3$ and also $N_1 \approx aN_z/(z_q - z_{q-1})$.

On the horizontal interface at z_q for $0 \le q \le Q$, we impose the continuity of tangential field components, i.e., the x and y components. We can write these conditions as

$$\hat{\mathbf{z}} \times \mathbf{E}(\mathbf{x}, z_q^-) = \hat{\mathbf{z}} \times \mathbf{E}(\mathbf{x}, z_q^+), \quad \mathbf{x} \in S_q, \tag{9}$$

$$\hat{\mathbf{z}} \times \mathbf{H}(\mathbf{x}, z_q^-) = \hat{\mathbf{z}} \times \mathbf{H}(\mathbf{x}, z_q^+), \quad \mathbf{x} \in S_q, \tag{10}$$

where $\hat{\mathbf{z}}$ is the unit vector in the positive z direction and S_0 (previously undefined) is taken to be S_1. At $z = z_0$, the spherical waves in the unit cell Ω_1 are required to match with the transmitted wave given in the plane wave expansion (4). In practice, we choose M_* uniformly distributed points in S_0 and require (9) and (10) for $q = 0$ to be valid at the M_* points. Similarly, at $z = z_Q = D$, the spherical waves in unit cell Ω_Q are required to match the sum of the incident and reflected waves given in (3), and the conditions (9) and (10) for $q = Q$ are imposed at M_* uniformly distributed point in S_Q.

If $1 \le q < Q$, the top surface of unit cell Ω_q may not coincide with the bottom surface of Ω_{q+1}, due to a possible horizontal shift of the centers of the spheres. That is, S_q is not identical to S_{q+1} if $\mathbf{s}_q \ne \mathbf{s}_{q+1}$. On the other hand, the entire xy plane can be filled by translations of S_q using the lattice vectors $\mathbf{a}_1$ and $\mathbf{a}_2$. Therefore, S_{q+1} can be divided into a few subdomains, where each subdomain corresponds to an integer pair (l_1, l_2). More precisely, the subdomain of S_{q+1} associated with (l_1, l_2) is the intersection of S_{q+1} with the shift of S_q by $l_1\mathbf{a}_1 + l_2\mathbf{a}_2$, i.e.,

$$\begin{aligned} S_{q+1}^{(l_1,l_2)} &= S_{q+1} \cap \{\mathbf{x} + l_1\mathbf{a}_1 + l_2\mathbf{a}_2 \mid \mathbf{x} \in S_q\} \\ &= \{\mathbf{x} + l_1\mathbf{a}_1 + l_2\mathbf{a}_2 \mid \mathbf{x} \in S_q^{(l_1,l_2)}\}. \end{aligned}$$

In the above, we have also defined a subdomain in S_q, i.e., $S_q^{(l_1,l_2)}$, which gives rise to $S_{q+1}^{(l_1,l_2)}$ when it is translated by $l_1\mathbf{a}_1 + l_2\mathbf{a}_2$. To impose the continuity conditions of the tangential field components, we need to apply the quasi-periodic conditions first. From (8), we obtain

$$\mathbf{E}(\mathbf{x} + l_1\mathbf{a}_1 + l_2\mathbf{a}_2, z) = \rho_1^{l_1}\rho_2^{l_2}\,\mathbf{E}(\mathbf{x}, z)$$

and a similar equation for $\mathbf{H}$. Therefore, (9) and (10) become

$$\rho_1^{l_1}\rho_2^{l_2}\,\hat{\mathbf{z}} \times \mathbf{E}(\mathbf{x}, z_q^-) = \hat{\mathbf{z}} \times \mathbf{E}(\mathbf{x} + l_1\mathbf{a}_1 + l_2\mathbf{a}_2, z_q^+), \tag{11}$$

$$\rho_1^{l_1}\rho_2^{l_2}\,\hat{\mathbf{z}} \times \mathbf{H}(\mathbf{x}, z_q^-) = \hat{\mathbf{z}} \times \mathbf{H}(\mathbf{x} + l_1\mathbf{a}_1 + l_2\mathbf{a}_2, z_q^+) \tag{12}$$

for $\mathbf{x} \in S_q^{(l_1,l_2)}$. An important case is when the shifts of the centers are given by

$$\mathbf{s}_q = \begin{cases} (0,0), & \text{if } q \text{ is odd;} \\ (\mathbf{a}_1 + \mathbf{a}_2)/2, & \text{if } q \text{ is even.} \end{cases} \tag{13}$$

For the square and equilateral triangular lattices given in (6) and (7), the centers of S_{q+1} is located at a corner of S_q, as shown in Fig. 1. For the square lattice, S_q and S_{q+1} have

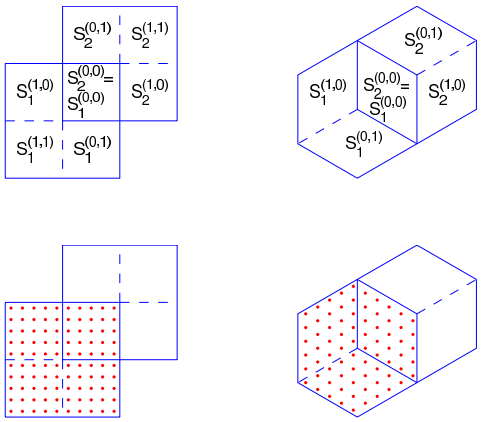

Fig. 1. Cross sections S_1 and S_2 of the first two unit cells Ω_1 and Ω_2, for square and triangular lattices, when the centers of spheres are shifted according to (13). The subdomains of S_1 and S_2 are needed for imposing the continuity conditions at $z = z_1$. Possible discretization points in S_1 are also shown.

four subdomains corresponding to $(l_1, l_2) = (0,0)$, $(0,1)$, $(1,0)$ and $(1,1)$. For the equilateral triangular lattice, S_q and S_{q+1} have three subdomains with $(l_1, l_2) = (0,0)$, $(0,1)$ and $(1,0)$. In the discrete case, when S_q and S_{q+1} are sampled by M_* points, (11) and (12) gives rise to $4M_*$ conditions. Clearly, the conditions (11) and (12) imply that the sampling points in $S_{q+1}^{(l_1,l_2)}$ must be obtained by translating the points in $S_q^{(l_1,l_2)}$ by $l_1\mathbf{a}_1 + l_2\mathbf{a}_2$. On the other hand, since S_q and S_{q+1} correspond to the same domain by different shifts, it is desirable if the sampling points in S_q and S_{q+1} are obtained from the same set of points using the two shifts $\mathbf{s}_q$ and $\mathbf{s}_{q+1}$. For an arbitrary $\mathbf{s}_{q+1} - \mathbf{s}_q$, this is difficult to achieve. For the square lattice and the shifts given in (13), this can be achieved if both S_q and S_{q+1} are sampled by $M_* = N_1^2$ uniformly distributed points and N_1 is even, as shown in Fig. 1. For the equilateral triangular lattice (7) and the shifts given in (13), we can also achieve this with a triangular distribution of the discrete points and using $M_* = 3N_1^2$ sampling points as shown in Fig. 1.

Overall, we obtain a system of equations for the reflection and transmission coefficients and the coefficients of the spherical waves in each unit cell. If we put the $2(2J_* + 1)^2$ coefficients of the transmitted wave in the column vector $\mathbf{d}_0$, the coefficients of the reflected wave in

$\mathbf{d}_{Q+1}$, and the $2L_*(L_*+2)$ coefficients of the spherical waves in Ω_q in column vector $\mathbf{d}_q$, then the system can be written as

$$\mathbf{A}\vec{\mathbf{d}} = \vec{\mathbf{f}}, \tag{14}$$

where

$$\mathbf{A} = \begin{bmatrix} A_{00} & A_{01} & & & & & \\ & \hat{A}_{11} & & & & & \\ & A_{11} & A_{12} & & & & \\ & & \hat{A}_{22} & & & & \\ & & \vdots & \ddots & & & \\ & & & \ddots & \vdots & & \\ & & & & \hat{A}_{QQ} & & \\ & & & & A_{QQ} & A_{Q,Q+1} \end{bmatrix}$$

and

$$\vec{\mathbf{d}} = \begin{bmatrix} \mathbf{d}_0 \\ \mathbf{d}_1 \\ \mathbf{d}_2 \\ \vdots \\ \mathbf{d}_Q \\ \mathbf{d}_{Q+1} \end{bmatrix}, \quad \vec{\mathbf{f}} = \begin{bmatrix} \mathbf{0} \\ \mathbf{0} \\ \vdots \\ \vdots \\ \mathbf{0} \\ \mathbf{f}_{2Q} \end{bmatrix}.$$

In the above, $A_{qq}\mathbf{d}_q + A_{q,q+1}\mathbf{d}_{q+1} = \mathbf{0}$ for $0 \le q < Q$, corresponds to the interface conditions at $z = z_q$. The last equation $A_{QQ}\mathbf{d}_Q + A_{Q,Q+1}\mathbf{d}_{Q+1} = \mathbf{f}_{2Q}$ corresponds to the interface conditions at $z = z_Q = D$. The non-zero right hand side comes from the incident wave. The equation $\hat{A}_{qq}\mathbf{d}_q = \mathbf{0}$ for $1 \le q \le Q$, corresponds to the quasi-periodic condtions on the lateral surfaces of Ω_q. Both A_{qq} and $A_{q,q+1}$ have $4M_*$ rows, where M_* is the number of points used to discretize S_q and S_{q+1}. The matrix $\hat{A}_{qq}$ has $4N_tN_z$ rows corresponding to the total number of quasi-peridic conditions imposed on the lateral surfaces of Ω_q. If the same number spherical waves and same number of discretization points are used for all unit cells, then the large coefficient matrix $\mathbf{A}$ has $4Q(M_* + N_tN_z) + 4M_*$ rows and $4(2J_*+1)^2 + 2QL_*(L_*+2)$ columns. If we attempt to keep the matrix $\mathbf{A}$ square by properly choosing the discretization points, then $\mathbf{A}$ is usually singular or very near singular. To obtain stable numerical solutions, it is necessary to choose the number of discretization points, so that the number of rows is 3 to 5 times larger than the number of columns, and then replace (14) by the least squares problem:

$$\min ||\mathbf{A}\vec{\mathbf{d}} - \vec{\mathbf{f}}||. \tag{15}$$

4. Improved solution technique

The standard procedure for solving the least squares problem is to use the QR decomposition of matrix $\mathbf{A}$ [19]. Since $\mathbf{A}$ has certain block bidiagonal form, we can use a recursive

method called sequential accumulation [19] to significantly reduce the required number of operations and the required computer memory. The method has been previously applied to this problem by Matsushima *et al.* [18]. To further speed up the method and reduce the memory requirement, we introduce some modifications to this method.

In our formulation, the unknown coefficients in $\vec{\mathbf{d}}$ are ordered from bottom ($z < 0$) to top ($z > D$), so that the coefficients of the reflected wave are given in the last block and the right hand side $\vec{\mathbf{f}}$ is non-zero (related to the incident wave) only in the last block. This is different from the formulation used in [18], where the first block of $\vec{\mathbf{f}}$ is non-zero. The advantage of our ordering is that when the sequential accumulation method is used, no work is needed for the right hand side until the final step.

Matsushima *et al.* [18] applied the sequential accumulation scheme to their least squares problem directly. We use a prepossessing step to reduce the size of the coefficient matrix, and then apply the sequential accumulation method to the smaller system. This allows us to reduce the required number of operations significantly if the total number of layers Q is large, especially when there are many identical layers in the structure. For $0 \le q \le Q$, we first calculate the following QR decomposition

$$\begin{bmatrix} A_{qq} & A_{q,q+1} \\ 0 & \hat{A}_{q+1,q+1} \end{bmatrix} = U_q \begin{bmatrix} B_{qq} & B_{q,q+1} \\ 0 & \hat{B}_{q+1,q+1} \\ 0 & 0 \end{bmatrix}, \tag{16}$$

where U_q is a unitary matrix, B_{qq} and $\hat{B}_{q+1,q+1}$ are square upper triangular matrices. Notice that the left hand side of (16) becomes $[A_{QQ}, A_{Q,Q+1}]$ if $q = Q$. The sizes of B_{qq} and $\hat{B}_{q+1,q+1}$ are related to the lengths of vectors $\mathbf{d}_q$ and $\mathbf{d}_{q+1}$. For $1 \le q < Q$, if the layers are identical, we have the same A_{qq}, $A_{q,q+1}$ and $\hat{A}_{q+1,q+1}$, thus the QR decomposition only has to be calculated once. The least squares problem (15) is then reduced to

$$\min ||\mathbf{B}\vec{\mathbf{d}} - \vec{\mathbf{g}}||, \tag{17}$$

where

$$\mathbf{B} = \begin{bmatrix} B_{00} & B_{01} & & & & & \\ & \hat{B}_{11} & & & & & \\ & B_{11} & B_{12} & & & & \\ & & \hat{B}_{22} & & & & \\ & & \vdots & \ddots & & & \\ & & & \ddots & \vdots & & \\ & & & & \hat{B}_{QQ} & & \\ & & & & B_{QQ} & B_{Q,Q+1} & \\ & & & & & \hat{B}_{Q+1,Q+1} \end{bmatrix}$$

and

$$\vec{\mathbf{g}} = \begin{bmatrix} \mathbf{0} \\ \mathbf{0} \\ \vdots \\ \vdots \\ \mathbf{0} \\ \mathbf{g}_{2Q} \\ \mathbf{g}_{2Q+1} \end{bmatrix}.$$

The sizes of blocks in $\vec{\mathbf{g}}$ follow the blocks in $\mathbf{B}$ and they are associated with the lengths of $\mathbf{d}_q$ for $0 \le q \le Q+1$. The last two non-zero blocks of $\vec{\mathbf{g}}$ are related to last block of $\vec{\mathbf{f}}$ by

$$U_Q^* \mathbf{f}_{2Q} = \begin{bmatrix} \mathbf{g}_{2Q} \\ \mathbf{g}_{2Q+1} \\ \vdots \end{bmatrix},$$

where U_Q^* is the conjugate transpose of U_Q. Since B_{qq} and $\hat{B}_{qq}$ are square matrices, the matrix $\mathbf{B}$ has $4(2J_*+1)^2+4QL_*(L_*+2)$ rows and $4(2J_*+1)^2+2QL_*(L_*+2)$ columns (same number of columns as $\mathbf{A}$). Notice that the size of $\mathbf{B}$ is independent of the discretization parameters N_z, M_*, N_1, etc. In particular, the number of rows of $\mathbf{B}$ is no more than twice the number of columns.

After the above prepossessing step, the sequential accumulation method is applied to the reduced least squares problem (17). The method involves the following steps.

1. Calculate the QR decomposition:

$$\begin{bmatrix} \hat{B}_{11} & 0 \\ B_{11} & B_{12} \end{bmatrix} = V_1 \begin{bmatrix} C_{11} & C_{12} \\ 0 & \hat{C}_{22} \\ 0 & 0 \end{bmatrix}.$$

2. For $2 \le q \le Q$, calculate the QR decomposition:

$$\begin{bmatrix} \hat{C}_{qq} & 0 \\ \hat{B}_{qq} & 0 \\ B_{qq} & B_{q,q+1} \end{bmatrix} = V_q \begin{bmatrix} C_{qq} & C_{q,q+1} \\ 0 & \hat{C}_{q+1,q+1} \\ 0 & 0 \end{bmatrix}.$$

3. Evaluate the vector

$$V_Q^* \begin{bmatrix} \mathbf{0} \\ \mathbf{0} \\ \mathbf{g}_{2Q} \end{bmatrix} = \begin{bmatrix} \mathbf{h}_Q \\ \hat{\mathbf{h}}_{Q+1} \\ \vdots \end{bmatrix}.$$

4. Calculate the QR decomposition

$$\begin{bmatrix} \hat{C}_{Q+1,Q+1} \\ \hat{B}_{Q+1,Q+1} \end{bmatrix} = V_{Q+1} \begin{bmatrix} C_{Q+1,Q+1} \\ 0 \end{bmatrix}.$$

5. Evaluate the vector

$$V_{Q+1}^{*}\begin{bmatrix}\hat{\mathbf{h}}_{Q+1}\\ \mathbf{g}_{2Q+1}\end{bmatrix}=\begin{bmatrix}\mathbf{h}_{Q+1}\\ \vdots\end{bmatrix}.$$

6. Solve $\vec{\mathbf{d}}$ from

$$\mathbf{C}\begin{bmatrix}\mathbf{d}_0\\ \mathbf{d}_1\\ \vdots\\ \mathbf{d}_Q\\ \mathbf{d}_{Q+1}\end{bmatrix}=\begin{bmatrix}\mathbf{0}\\ \mathbf{0}\\ \vdots\\ \mathbf{h}_Q\\ \mathbf{h}_{Q+1}\end{bmatrix}, \tag{18}$$

where

$$\mathbf{C}=\begin{bmatrix}B_{00} & B_{01} & & & & \\ & C_{11} & C_{12} & & & \\ & & \ddots & \ddots & & \\ & & & C_{QQ} & C_{Q,Q+1} & \\ & & & & C_{Q+1,Q+1} & \end{bmatrix}.$$

In the above, V_q, for $1 \le q \le Q+1$, are unitary matrices, C_{qq} for $1 \le q \le Q+1$ and $\hat{C}_{qq}$ for $2 \le q \le Q+1$, are square upper triangular matrices. The sizes of C_{qq} and $\hat{C}_{qq}$ are compatible with the vector $\mathbf{d}_q$. The vector $\mathbf{h}_Q$ has the same length as $\mathbf{d}_Q$. The vectors $\hat{\mathbf{h}}_{Q+1}$ and $\mathbf{h}_{Q+1}$ have the same length as $\mathbf{d}_{Q+1}$. V_Q^* is the conjugate transpose of V_Q, etc. Since $\mathbf{f}$ is non-zero only in its last block, the unitary matrices U_q and V_q for $q < Q$, are not needed. Therefore, the standard algorithm for computing the QR decomposition may be modified to avoid computing these unitary matrices. Due to the sequential nature of the method, the required computation time is linearly proportional to the total number of layers, i.e., Q. The linear system (18) can be easily solved by backward substitution. In that case, the required computer memory is also proportional to Q.

For large Q, we propose an alternative method that requires much less computer memory. In fact, the required memory of the our method is independent of Q. Obviously, if we only want to calculate the reflected wave, there is no need to store the matrices B_{00}, B_{01}, C_{qq} and $C_{q,q+1}$ for $q \le Q$. We only need to solve $\mathbf{d}_{Q+1}$ from the last equation of (18), i.e.,

$$C_{Q+1,Q+1}\mathbf{d}_{Q+1}=\mathbf{h}_{Q+1}.$$

To calculate the transmitted wave with reduced memory, we introduce the matrix Y_q satisfying

$$\mathbf{d}_0 = Y_q\mathbf{d}_q$$

for $0 \le q \le Q$. From (18), it is easy to see that

$$\begin{aligned} Y_1 &= -B_{00}^{-1}B_{01}, \\ Y_{q+1} &= -Y_qC_{qq}^{-1}C_{q,q+1}, \quad q=0,1,...,Q-1. \end{aligned}$$

The above formulas for Y_1 and Y_{q+1} can be inserted into the first and second steps of the sequential accumulation algorithm described earlier. After the fifth step is completed, we solve $\mathbf{d}_{Q+1}$ and $\mathbf{d}_Q$ from the last two equations of (18), then evaluate $\mathbf{d}_0 = Y_Q \mathbf{d}_Q$.

5. Numerical examples

In this section, we present some numerical examples. First, we consider four layers of spheres (i.e. $Q = 4$), where each layer consists of dielectric spheres on a square lattice with a lattice constant a. The spheres in all layers are identical. The radius and the dielectric constant of the spheres are $0.2a$ and $\varepsilon = 10$, respectively. The medium outside the spheres is air. All layers have the same thickness which is equal to a, thus $z_q = qa$ for $0 \le q \le Q$ and $D = z_Q = 4a$. The centers of the spheres in each layer are located on the middle plane parallel to the xy plane. Therefore, the z coordinates of the spheres in the q-th layer (given by $z_{q-1} < z < z_q$) is $z_{q-1/2} = (q - 1/2)a$. We consider two cases. In the first case, the centers of the spheres in different layers are not shifted, i.e., $\mathbf{s}_q = (0, 0)$ for $1 \le q \le Q$. Thus, the spheres actually form a simple cubic lattice. In the second case, we let the centers of the spheres to shift half a lattice constant in both periodic directions, as given in (13). For a normal incident wave, i.e., $\vec{\alpha}_0 = (0, 0)$, we calculate the power carried by the $(0, 0)$-th transmitted diffraction order. Our results are shown in Fig. 2, and they are obtained by truncating the plane wave expansions of the reflected and transmitted waves with $J_* = 5$, and truncating the spherical wave expansions in each unit cell with $L_* = 15$. The unit cell Ω_q (for $1 \le q \le Q$) is a cube with edges of length a. For the results in Fig. 2, we have used 14 points to discretize any distance of length a. Therefore, $N_z = N_1 = N_2 = 14$, $N_t = 2 \times 14 = 28$ and $M_* = 14^2 = 196$. The first case has been previously analyzed by Matsushima *et al.* [18]. Their results are nearly identical to ours, but the two narrow spikes for $\omega a/(2\pi c)$ near 0.779 and 0.926 are missing. Most likely, this is due to a coarser sampling of the frequency. The two cases (with or without shifts) show some difference in the transmission spectra, but the main features, such as the frequency intervals for low transmission, are quite close.

Next, we consider one layer of air spheres in a dielectric slab having a dielectric constant $\varepsilon = 2.72$. The air spheres in the slab form a square lattice with lattice constant a. The radius of the spheres is $0.2a$. The slab containing the air spheres is given by $0 < z < D = a$. The centers of the air spheres are located on the plane at $z = a/2$. Outside the slab, i.e. for $z < 0$ and $z > D$, the medium is air. For this structure, we obtain the transmission spectrum shown in Fig. 3 using the same truncation orders and discretization parameters, i.e., $J_* = 5$, $L_* = 15$, and $N_z = 14$, etc. The results are obtained for a normal incident wave. Since the dielectric constant of the slab is not so high, the transmission coefficient is typically quite large, but there are a few narrow dips in the spectra. Since the structure is lossless, these dips correspond to high reflectivity.

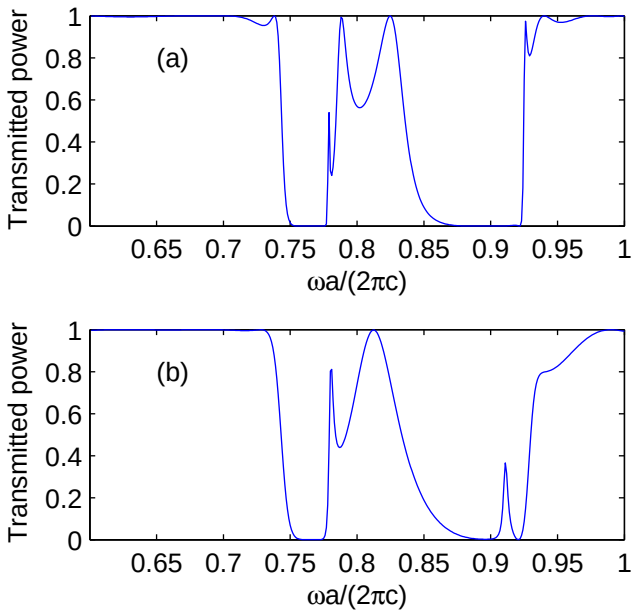

Fig. 2. Transmission spectra of a normal incident plane wave for four layers of dielectric spheres. The spheres in each layer are located on a square lattice. (a) The centers of the spheres are not shifted. (b) The centers of the spheres are shifted according to (13).

Finally, we consider four layers of dielectric spheres, where the spheres in each layer are given on an equilateral triangular lattice with lattice constant a. As in the first example, we assume that the spheres have a radius $0.2a$ and a dielectric constant $\varepsilon = 10$, and they are surrounded by air. We consider two cases. In the first case, the spheres in different layers are not shifted and the thickness of each layer is a. In the second case, the spheres are shifted according to (13) and the thickness of each layer is $\sqrt{2/3}\,a$. For both cases, we specify a normal incident wave with an electric field $\mathbf{E}^{(i)}$ parallel to the x axis. The transmission spectra of these two cases are shown in Fig. 4. Although both cases have four identical layers of spheres, their transmission spectra are quite different. These results are obtained with the truncation orders $J_* = 5$ and $L_* = 15$, and the discretization parameters $N_1 = N_2 = N_3 = 8$, $N_t = 3 \times 8 = 24$ and $M_* = 3 \times 8^2 = 192$. Due to the difference in layer thickness, we used $N_z = 14$ and $N_z = 11$ for the first and second cases, respectively.

For the examples presented earlier, we have performed some numerical convergence tests. As a typical example, we consider the second case above for spheres on the triangular lattice with shifts and $\omega a/(2\pi c) = 0.85$. For a number of truncation and discretization parameters,

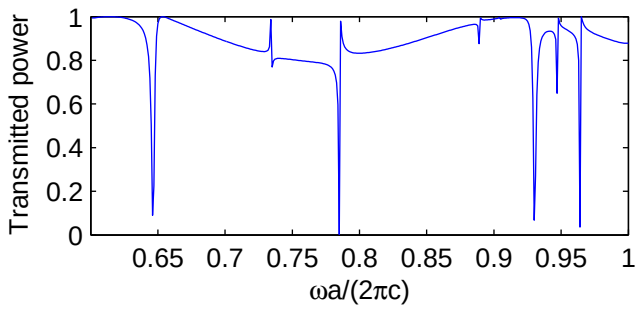

Fig. 3. Transmission spectrum of a normal incident plane wave for a dielectric slab containing air shperes on a square lattice with lattice constant a. The thickness of the slab is also a.

we calculate the transmited and reflected powers, relative to the power of the normal incident plane wave. Our results are given in Table 1, where T.P. $= |\mathbf{R}_{00}|^2 + |\mathbf{T}_{00}|^2$ is the total power.

J_*	N_1	N_z	$\lvert\mathbf{R}_{00}\rvert^2$	$\lvert\mathbf{T}_{00}\rvert^2$	T.P.
3	5	7	0.334190	0.660907	0.995097
4	7	10	0.334636	0.663966	0.998602
5	8	11	0.334759	0.665194	0.999953
6	10	14	0.334688	0.665309	0.999997
7	11	16	0.334693	0.665307	1.000000

Table 1. Reflected and transmitted powers of a normal incident plane wave for four layers of dielectric spheres and $\omega a/(2\pi c) = 0.85$, calculated using different truncation and discretization parameters. The spheres in each layer are located on a triangular lattice of lattice constant a. The centers of the spheres are shifted according to (13) and the thickness of the layers is $\sqrt{2/3}\,a$.

The other parameters are $L_* = 3J_*$, $N_t = 3N_1$, $N_2 = N_3 = N_1$ and $M_* = 3N_1^2$. Since the $(0,0)$-th diffraction order is the only propagating mode, and the media in $z < 0$ and $z > D$ are the same, the squared magnitudes of vectors $\mathbf{R}_{00}$ and $\mathbf{T}_{00}$ represent the relative powers of the reflected and transmitted waves, respectively. From Table 1, we observe that as the truncation orders and the discretization parameters increase accordingly, the numerical results appear to converge and the power balance law is satisfied.

Although the numerical examples in this section involve only normal incident waves and dielectric media, our method is applicable to incident waves with arbitrary angles of incidence

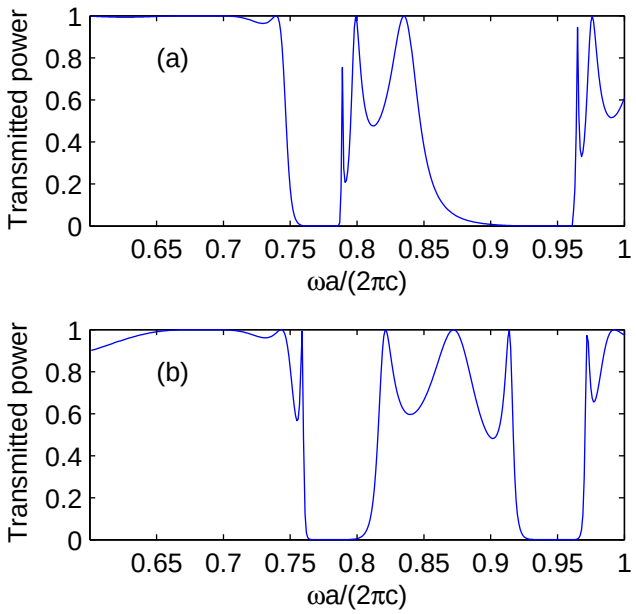

Fig. 4. Transmission spectra of a normal incident plane wave for four layers of dielectric spheres. The spheres in each layer are located on a triangular lattice with lattice constant a. (a) The centers of the spheres are not shifted and the thickness of the layers is a. (b) The centers of the spheres are shifted according to (13) and the thickness of the layers is $\sqrt{2/3}\,a$.

and to metallic structures. As in other methods based on spherical wave expansions, the convergence slows down and the method becomes more expensive when the radius of the spheres is increased.

6. Conclusion

In this paper, we extended the spherical wave least squares method developed by Matsushima *et al.* [18] for arrays of spheres on a simple cubic lattice to general periodic multilayer structures where each layer consists of an array of spheres on an arbitrary 2D lattice. In different layers, the spheres and the media outside the spheres can be different. The centers of the spheres in different layers can have different shifts parallel to the plane of periodicity. We also developed new solution techniques to significantly reduce the required number of operations and the required computer memory. The method can be regarded as an alternative to the layer-KKR method [6, 7] which requires complicated manipulations of the spherical wave functions and evaluating the lattice sums. In our method, spherical wave expansions

are only used in one unit cell for each layer. The multiple scattering effect due to the infinite number of spheres in the layer is handled by imposing quasi-periodic conditions on the lateral surfaces of the unit cell in the least squares sense. Since the method is quite simple, it can be easily modified for different physical and geometric configurations.

Appendix

Spherical waves are special solutions of the Maxwell's equations (1) for a homogeneous sphere centered at the origin and embedded in a homogeneous medium. They are usually given in the spherical coordinate system (r, θ, ϕ). For each integer pair (l, m) satisfying $l \geq 1$ and $-l \leq m \leq l$, there are two linearly independent spherical waves. If the radius of the sphere is a, the relative permittivity and magnetic permeability of the sphere and the surrounding medium are $\{\varepsilon_1, \mu_1\}$ and $\{\varepsilon_2, \mu_2\}$, respectively, then there are two functions $\psi^{(1)}$ and $\psi^{(2)}$ of the radial variable r given by

$$\psi^{(p)}(r) = \begin{cases} c^{(p)} j_l(k_1 r), & \text{if } r < a, \\ a^{(p)} j_l(k_2 r) + b^{(p)} h_l^{(1)}(k_2 r), & \text{if } r > a, \end{cases}$$

for $p = 1, 2$, where $k_1 = k_0\sqrt{\varepsilon_1\mu_1}$, $k_2 = k_0\sqrt{\varepsilon_2\mu_2}$, j_l and $h_l^{(1)}$ are spherical Bessel and Hankel functions defined as

$$j_l(\tau) = \sqrt{\frac{\pi}{2\tau}} J_{l+\frac{1}{2}}(\tau), \quad h_l^{(1)}(\tau) = \sqrt{\frac{\pi}{2\tau}} H_{l+\frac{1}{2}}^{(1)}(\tau).$$

Given $c^{(p)}$, the coefficients $a^{(p)}$ and $b^{(p)}$ can be solved from the conditions that $\psi^{(p)}$, $\varepsilon^{-1}\partial_r[r\psi^{(1)}]$ and $\mu^{-1}\partial_r[r\psi^{(2)}]$ are continuous at $r = a$. For an integer m satisfying $|m| \leq l$, we let

$$\Psi^{(p)}(r, \theta, \phi) = \psi^{(p)}(r) Y_l^m(\theta, \phi),$$

where Y_l^m is the spherical harmonic given by

$$Y_l^m(\theta, \phi) = \left[\frac{(2l+1)(l-m)!}{4\pi(l+m)!}\right]^{1/2} P_l^m(\cos\theta)\, e^{im\phi},$$

P_l^m is the associated Legendre polynomial and $Y_l^{-m} = (-1)^m \overline{Y_l}^m$, then the two spherical waves are

$$\begin{aligned} E_r^{(1)} &= \frac{-l(l+1)}{ik_0\varepsilon r}\Psi^{(1)}, \\ E_\theta^{(1)} &= \frac{-1}{ik_0\varepsilon r}\frac{\partial^2[r\Psi^{(1)}]}{\partial r \partial\theta}, \\ E_\phi^{(1)} &= \frac{-1}{ik_0\varepsilon r\sin\theta}\frac{\partial^2[r\Psi^{(1)}]}{\partial r \partial\phi}, \\ H_r^{(1)} &= 0, \end{aligned}$$

$$
\begin{aligned}
H_\theta^{(1)} &= \frac{1}{\sin\theta}\frac{\partial \Psi^{(1)}}{\partial \phi}, \\
H_\phi^{(1)} &= -\frac{\partial \Psi^{(1)}}{\partial \theta},
\end{aligned}
$$

and

$$
\begin{aligned}
E_r^{(2)} &= 0, \\
E_\theta^{(2)} &= \frac{1}{\sin\theta}\frac{\partial \Psi^{(2)}}{\partial \phi}, \\
E_\phi^{(2)} &= -\frac{\partial \Psi^{(2)}}{\partial \theta}, \\
H_r^{(2)} &= \frac{l(l+1)}{ik_0\mu r}\Psi^{(2)}, \\
H_\theta^{(2)} &= \frac{1}{ik_0\mu r}\frac{\partial^2[r\Psi^{(2)}]}{\partial r \partial \theta}, \\
H_\phi^{(2)} &= \frac{1}{ik_0\mu r\sin\theta}\frac{\partial^2[r\Psi^{(2)}]}{\partial r \partial \phi}.
\end{aligned}
$$

In the above, $\varepsilon = \varepsilon_1$ if $r < a$ and $\varepsilon = \varepsilon_2$ if $r > a$, and μ is similarly defined.

Acknowledgments

This research was partially supported by a grant from the Research Grants Council of Hong Kong Special Administrative Region, China (Project No. CityU 102008).

References

1. J. D. Joannopoulos, R. D. Meade, and J. N. Winn, *Photonic Crystals: Molding the Flow of Light*, Princeton University Press, Princeton, NJ. 1995.
2. K. M. Ho, C. T. Chan, and C. M. Soukoulis, "Existence of a photonic gap in periodic dielectric structures," Phys. Rev. Lett. **65**, 3152-3155 (1990).
3. E. Yablonovitch, T. J. Gmitter, and K. M. Leung, "Photonic band structure: The face-centered-cubic case employing nonspherical atoms," Phys. Rev. Lett. **67**, 2295-2298 (1991).
4. K. M. Ho, C. T. Chan, C. M. Soukoulis, R. Biswas, and M. Sigalas, "Photonic band gaps in three dimensions: New layer-by-layer periodic structures," Solid State Communications **89**, 413-416 (1994).
5. H. S. Sözüer and J. P. Dowling, "Photonic band calculations for woodpile structures," J. Mod. Opt. **41**, 231-239 (1994).
6. K. Ohtaka, "Scattering theory of low-energy photon diffraction," Journal of Physics C: Solid State Physics **13**, 667-680 (1980).

7. A. Modinos, "Scattering of electromagnetic waves by a plane of spheres – formalism," Physica A **141**, 575-588 (1987).
8. P. A. Martin, *Multiple Scattering: Interaction of Time-Harmonic Waves with N Obstacles*, Cambridge Univeristy Press, Cambridge, UK. 2006.
9. M. Born and E. Wolf, *Principles of Optics*, 7th ed., Cambridge Univeristy Press, Cambridge, UK. 1999.
10. N. Stefanou and A. Modinos, "Scattering of light from a two-dimensional array of spherical particles on a substrate," Journal of Physics: Condensed Matter **3**, 8135-8148 (1991).
11. N. Stefanou, V. Karathanos, and A. Modinos, "Scattering of electromagnetic waves by periodic structures," Journal of Physics: Condensed Matter **4**, 7389-7400 (1992).
12. K. Ohtaka and Y. Tanabe, "Photonic bands using vector spherical waves. II. Reflectivity, coherence and local field," Journal of the Physical Society of Japan **65**, 2276-2284 (1996).
13. N. Stefanou, V. Yannopapas, and A. Modinos, "Heterostructures of photonic crystals: frequency bands and transmission coefficients," Computer Physics Communications **113**, 49-77 (1998).
14. N. Stefanou, V. Yannopapas, and A. Modinos, "MULTEM 2: A new version of the program for transmission and band-structure calculations of photonic crystals," Computer Physics Communications **132**, 189-196 (2000).
15. L. Li, "New formulation of the Fourier modal method for crossed surface-relief gratings," J. Opt. Soc. Am. A **14**, 2758-2767 (1997).
16. G. Bao, P. Li, and H. Wu, "An adaptive edge element method with perfectly matched absorbing layers for wave scattering by biperiodic structures," Mathematics of Computation **70**, 1-34 (2010).
17. E. Popov and M. Nevière, "Maxwell equations in Fourier space: A fast-converging formulation for diffraction by arbitrary shaped, periodic, anisotropic media," J. Opt. Soc. Am. A **18**, 2886-2894 (2001).
18. A. Matsushima, Y. Momoka, M. Ohtsu, and Y. Okuno, "Efficieint numerical approach to electromagnetic scattering from three-dimensional periodic array of dielectric spheres using sequential accumulation," Progress in Electromagnetics Research **69**, 305-322 (2007).
19. C. L. Lawson and R. J. Hanson, Solving Least Squares Problems, SIAM, Philadelphia, PA, 1995.